Measurement of 1-ps soft-x-ray laser pulses from an injection-seeded plasma amplifier

Y. Wang,[1] M. Berrill,[1] F. Pedaci,[1] M. M. Shakya,[2] S. Gilbertson,[2] Zenghu Chang,[2] E. Granados,[1] B. M. Luther,[1] M. A. Larotonda,[1] and J. J. Rocca[1,3]

[1]*NSF ERC for Extreme Ultraviolet Science and Technology and Department of Electrical and Computer Engineering, Colorado State University, Fort Collins, Colorado 80523, USA*

[2]*J.R. Macdonald Laboratory, Department of Physics, Kansas State University, Manhattan, Kansas 66506, USA*

[3]*Department of Physics, Colorado State University, Fort Collins, Colorado 80523, USA*

(Received 11 May 2008; published 6 February 2009)

We report on a pulsewidth measurement of phase-coherent soft x-ray laser pulses generated by injection seeding a solid-target plasma amplifier with high harmonic pulses. A pulse duration of 1.13 ± 0.47 ps was measured for a seeded Ne-like Ti plasma amplifier operating at 32.6 nm using an ultrafast streak camera. This is the shortest pulse duration reported to date from a table-top soft x-ray laser amplifier. The result agrees with model simulations which suggest that intense femtosecond soft x-ray laser pulses could be obtained by injection seeding a tailored plasma amplifier in which the gain is confined to a high density region.

DOI: 10.1103/PhysRevA.79.023810 PACS number(s): 42.55.Vc, 42.60.By, 52.38.Ph

Table-top soft x-ray lasers based on the amplification of spontaneous emission in plasma amplifiers produce energetic laser pulses whose duration is determined by the duration of the gain. Compact soft x-ray lasers generating intense pulses of light with a duration ranging from 5 ps to nanoseconds have been used in the past several years for a wide range of applications that include dense plasma diagnostics [1,2], soft x-ray microscopy [3,4], paraelectric-ferroelectric phase transition studies [5], nanopatterning [6], photoelectron emission studies of surfaces [7], and nanocluster mass spectroscopy studies [8,9]. There is keen interest in reducing the pulse duration of table-top soft x-ray lasers to extend their application to a wide range of ultrafast dynamic studies. Transient inversions created by rapid heating of plasmas with intense picosecond optical laser pulses have generated soft x-ray laser pulses with duration between 2 and 10 ps at a rate of a pulse every several minutes [10–13]. High repetition rate transient inversion lasers produced by grazing incidence pumping have been measured to produce pulse duration of about 5 ps [14]. In all these soft x-ray lasers the pulse duration was determined by the duration of the gain. The recent demonstration of injection-seeded soft x-ray lasers [15–19] creates a fundamentally unique regime for the generation of short soft x-ray laser pulses in which the pulsewidth is governed by the amplifier bandwidth and is independent of the gain duration. In those experiments high harmonic (HH) pulses were amplified in laser transitions from multiply charged ions in plasmas created by either optical field ionization of gaseous media [15] or by laser irradiation of solid targets [16–19]. The higher density of the latter gain media results in broader laser line bandwidths that can support the generation of shorter soft x-ray laser pulses. The amplification of HH pulses in soft x-ray laser amplifiers created by irradiating solid targets has been modeled [16,17,20], but a measurement of the pulsewidth has not been available for comparison.

In this paper we report on a measurement of the duration of phase-coherent soft x-ray laser pulses from an injection-seeded plasma amplifier created by irradiating a solid target. An ultrafast streak camera was used to make single-shot measurements of soft x-ray pulses generated by seeding the 32.6 nm line of Ne-like Ti with the 25th harmonic of a Ti:sapphire laser. The measured pulse duration of 1.13 ± 0.47 ps is the shortest soft x-ray pulse duration demonstrated to date from a plasma amplifier. The results are compared with hydrodynamic/atomic physics model computations that show that injection seeding of denser plasmas with a tailored gain profile will lead to femtosecond soft x-ray lasers. We propose a seeded amplifier design for the generation of ~300 fs pulses at 10.9 nm.

The setup of the experiment is schematically illustrated in Fig. 1. High-resolution single-shot laser pulse measurements were made possible by an electrostatically focused ultrafast soft x-ray streak camera. The camera made use of a transmission photocathode consisting of a 100-nm-thick layer of KBr deposited onto a 150-nm-thick Al foil. The camera can reach a resolution of ~0.3 ps when an additional slit is introduced in the photoelectron path to limit the deflection aberration caused by the lateral electron velocity spread [21]. However, since for accurate single-shot measurements the use of the slit would require an increase in the number of electrons leaving the photocathode, which would increase space charge and degrade the camera resolution, the slit was not used in these measurements. Measurements of the streak camera resolution in this configuration are presented below. The soft x-ray laser amplifier consisted of a 3-mm-long Ti plasma column producing gain in the 32.6 nm $J=0-1$ line of Ne-like Ti. A description of the characteristics of such a Ne-like titanium amplifer can be found in Ref. [22]. This tran-

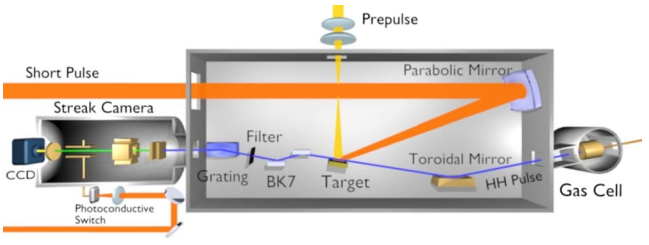

FIG. 1. (Color online) Schematic representation of the setup used to generate and measure the duration of soft x-ray laser pulses from an injection-seeded Ne-like Ti soft x-ray laser.

sient gain amplifier plasma was created by laser heating a polished Ti slab with pulses from a table-top Ti:sapphire laser operating at 800 nm. The amplifier was seeded with pulses from the 25th harmonic of the same laser to produce phase-coherent soft x-ray pulses with energies up to 60 nJ [16]. The HH seed pulses were generated by focusing into an argon gas cell 20 mJ pulses from the same Ti:sapphire laser, separately compressed to ~50 fs. The HH output of the gas cell was relay imaged onto a ~100 μm diameter spot at the input of the plasma amplifier using a gold-coated toroidal mirror designed to operate at a grazing incidence angle of 10°. The wavelength of the selected HH order was made to overlap with that of the laser line tuning a thin etalon introduced in the first of the three multipass amplifiers of the Ti:sapphire laser system. The Ti soft x-ray amplifier was excited with a sequence of a 10 mJ prepulse of 120 ps duration, followed after about 5 ns by a second prepulse of the same duration and ~350 mJ energy impinging at normal incidence, which in turn was followed after 500 ps by ~0.9 J heating pulse of 6.7 ps duration impinging at a grazing incidence angle of 23°. This grazing incidence pumping geometry takes advantage of the refraction of the pump beam to increase the energy deposition in the plasma region with optimum density for amplification [23,24]. The 23° angle was selected to couple the pump beam into the region where the plasma density is $\sim 2.7 \times 10^{20}$ cm^{-3}. The remaining part of the Ti:sapphire laser beam used to generate the high harmonics was attenuated using two BK7 windows positioned at 9° grazing incidence and a set of two 0.3-μm-thick aluminum filters. The output of the soft x-ray amplifier was dispersed with a variable space diffraction grating (nominal line spacing 1200 lines/mm) and directed toward the streak camera. It should be noticed that in the current setup the diffraction grating does not significantly broaden the pulse. This results from the fact that the 20 micrometer wide input slit of the streak camera was placed at 14 cm from the image plane of the variable space grating, which reduces the time delay dispersion to about 80 fs. The streak camera was synchronized with the soft x-ray laser pulse by closing a photoconductive switch that generates the voltage ramp using a 50 fs, ~80 μJ light pulse from the same Ti:sapphire laser.

A detailed time-dependent simulation of the electron trajectories in the streak camera tube show that for accurate single-shot pulsewidth measurements the number of photoelectrons reaching the screen must fall within a relatively narrow range. On one side a high number of photoelectrons creates a space charge that can significantly broaden the pulse. To reduce its effect we pulsed-biased the photocathode at −12 kV, an acceleration potential that is significantly higher than the −7 kV at which the camera is normally operated in synchroscan mode [21]. However, detailed model simulations of the streak camera response show that even at this high acceleration voltage the number of photoelectons detected by the camera's multichannel plate screen must remain below about 50 in order to avoid significant space charge broadening of the pulse. On the other hand, if the number of photoelectrons reaching the screen is very low (e.g., 10) their statistical spread causes a large uncertainty in the determination of the pulsewidth. Furthermore, it can be shown that when the number of detected photoelectrons is low, the probability that the tails of the pulse are properly sampled is reduced causing the pulsewidth to be systematically underestimated (e.g., by 20% for a 1.1 ps wide pulse if only ten photoelectrons are detected). For these reasons we used streaks in which the number of detected photoelectrons was between 20 and 50. The model simulations showed, as corroborated by the experimental results, that for less than 50 photoelectrons the space charge-induced pulse broadening is significantly smaller than the broadening resulting from the electron velocity spread at the photocathode. Moreover, the simulations of the electron trajectories in the streak tube show that since the space charge broadening affects the streak camera resolution measurements approximately as much as it affects the laser pulsewidth measurements, the effect of the space charge should cancel on the final pulsewidth measurement. This is corroborated by the experimental results discussed below, that yield pulsewidth values that are independent of the number of photoelectrons when their number is within the range mentioned above.

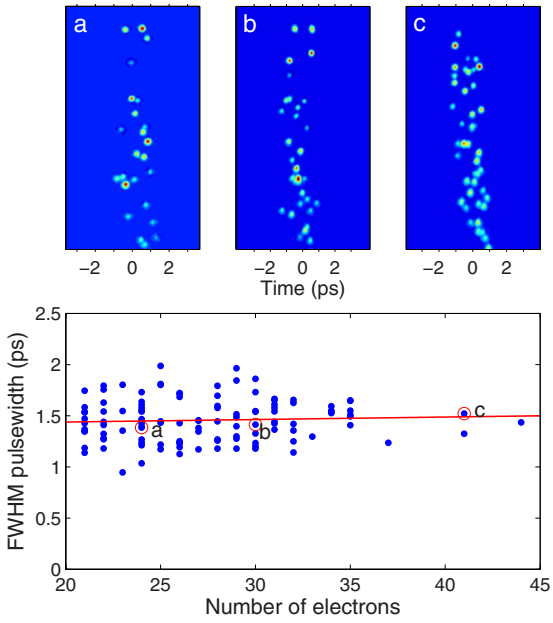

FIG. 2. (Color online) Top: Examples of single-shot streaks of high harmonic pulses used to determine the resolution of the camera. The vertical axis is in the direction of the slit. Bottom: measured pulsewidth as a function of number of photoelectrons recorded on the camera screen. The letters identify the individual streaks shown on the top of the figure.

The resolution of the camera was determined *in situ* by measuring the pulse duration of the HH seed pulse, whose pulse duration of ~50 fs is much shorter than the camera resolution. The upper part of Fig. 2 shows the distribution of detected photoelectrons at the camera screen for three typical single-shot HH streaks. Each spot is caused by the arrival of a single electron to the camera screen followed by amplification in the microchannel plate. The plot in the lower part of Fig. 2 shows the measured pulsewidth, which is in effect the camera resolution, as a function of the number of detected photoelectrons in the range of 20–50. Here the pulsewidth is defined as the time interval containing 76% of the electrons,

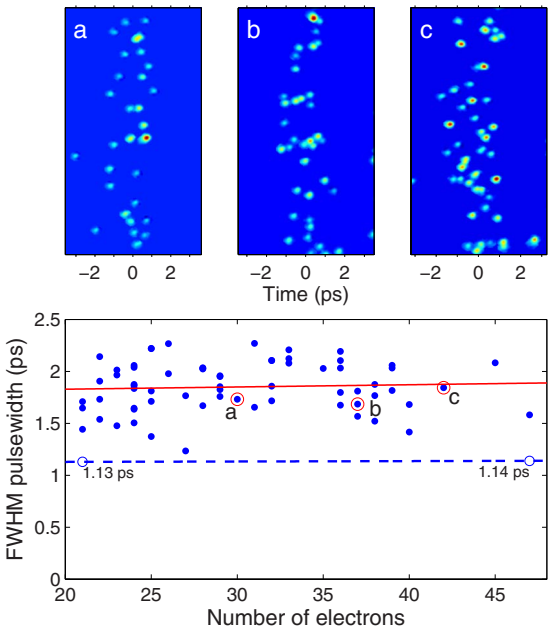

FIG. 3. (Color online) Top: Examples of single-shot streak-camera measurements of the amplified seed pulses. The vertical axis is in the direction of the slit. Bottom: Recorded seeded laser pulsewidth as a function of number of photoelectrons recorded on the camera screen. The solid line is a linear fit to the data. The dashed line is the deconvoluted real pulsewidth as a function of the number of electrons calculated from the linear fits to the data in Figs. 2 and 3. The resulting measured pulsewidth is 1.13 ± 0.47 ps.

corresponding to the full width at half maximum of a Gaussian distribution. A linear least square fit of the data shows that the pulsewidth slightly increases as a function of the number of detected photoelectrons. The numerical simulations of the camera response shows that this effect is dominantly caused by the slightly larger undersampling error at low number of detected photoelectrons, and that the spread of the pulsewidth data is dominated by the statistical energy distribution of the electrons emitted by the photocathode. Figure 3 summarizes the streak camera measurement of the amplified seed pulses. The frames on the upper part of the figure show three individual streaks. The linear fit of the measured pulsewidth dependence as a function of detected photoelectron number shows again a small positive slope. The pulsewidth of the seeded laser T_p can be obtained from the data in Figs. 2 and 3 by deconvolution using $T_p = \sqrt{T_m^2 - T_{\mathrm{HH}}^2}$, where T_m and T_{HH} are the measured seeded laser pulsewidth and the streak camera resolution determined by the measurement of the HH pulsewidth shown in Fig. 2, respectively. The result of the deconvolution is the dashed line shown at the bottom of Fig 3. The flat slope shows that the resulting seeded laser pulsewidth is independent from the number of detected photoelectrons, as the systematic error caused by undersampling in T_m and T_{HH} practically cancels. The resulting laser pulsewidth of 1.13 ± 0.47 ps is to our knowledge the shortest x-ray laser pulse generated to date from a plasma amplifier. The uncertainty was estimated by error propagation assuming that the error in the measured values of T_m and T_{HH} corresponds to their standard deviation.

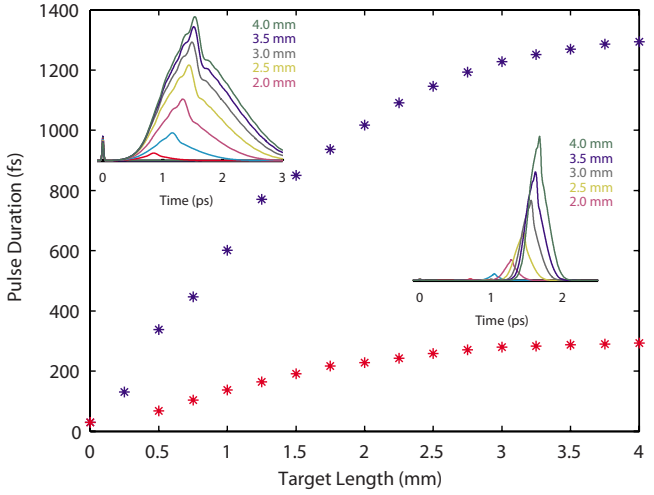

FIG. 4. (Color online) Upper (blue) curve: Simulated variation of the seeded Ne-like Ti laser pulsewidth as a function of amplifier length. In the first 2 mm of the amplifier rapid line narrowing of the amplified seed pulse results in a temporally broader pulse. In the last 2 mm the pulse broadens due to both additional line narrowing and gain saturation. The pulsewidth is defined as the time interval that contains 76% of the pulse energy, corresponding to the FWHM of a Gaussian distribution. The left inset shows the computed temporal profiles of the amplified seed pulse as a function of amplifier length. The proceeding short pulse contains the nonamplified frequencies of the injected seed. Lower (red) curve: Simulated variation of the pulsewidth of a HH seed into a dense Ni-like Te amplifier for the conditions specified in the text. The right inset shows the computed temporal profiles for these conditions.

The measured laser pulse duration is in good agreement with model simulations of the seed amplification. The simulations were performed using a 3D propagation code that self-consistently computes the seed intensity increase and the gain saturation due to population inversion depletion by both the amplified spontaneous emission and the amplified seed pulse in a fully transient approach. A $1\frac{1}{2}D$ Lagrangian hydrodynamic code coupled to a transient collisional-radiative atomic physics model was used to calculate the plasma parameters [25]. Figure 4 shows the simulated variation of the amplified seed pulsewidth as a function of plasma amplifier length. Initially, the seed pulse broadens as its bandwidth narrows dramatically in the much narrower bandwidth plasma amplifier. Subsequently, the simulations indicate that as the amplified seed pulse approaches the saturation fluence at about 2.5 mm within the amplifier the effect of gain saturation starts to contribute to additional pulse broadening. The pulsewidth is computed to increase from ~ 1.0 ps at 2 mm to 1.3 ps at 4 mm, an increase caused by additional line narrowing and saturation broadening. The simulated pulse duration of 1.2 ps at 3 mm is in good agreement with the measured pulsewidth. The bandwidth of the amplified seed pulse at this point is computed to be 3.6×10^{11} Hz. As a result the computed time-bandwidth product is 0.43, close to the transform-limited value of 0.36 for our Voigt profile.

Moreover, soft x-ray laser pulse durations of a few hundred femtoseconds should be achieved by seeding an amplifier in which gain takes place in a higher density region

where collisional broadening increases the amplifier bandwidth. For example, simulations suggest gain-saturated laser pulses of ~290 fs duration could be obtained seeding a 3.5-mm-long $\lambda=10.9$ nm Ni-like Te plasma amplifier with an electron density of $\sim 2\times 10^{21}$ cm^{-3}. The simulations show that gain at that density can be produced in a region with a sufficiently low density gradient to limit refraction by focusing a sequence of three frequency doubled ($\lambda=400$ nm) Ti:sapphire laser pulses onto the target at normal incidence to form a 30 μm$\times$4 mm line. The first pulse (200 mJ, 120 ps duration) creates a plasma that is allowed to expand for 2 ns to reduce the density gradient. The second pulse of the sequence (1 J, 120 ps) ionizes the plasma to the Ni-like state. A traveling wave configuration is used for the third pulse (1 J, 6 ps) that arrives 100 ps after the peak of the second pulse to rapidly heat the plasma to ~350 eV. This produces a transient gain of $g\sim 80-110$ cm^{-1} in the dense plasma region where the laser transition has a linewidth of $\Delta\nu \sim 4-8\times 10^{12}$ Hz that can support the amplification of a short pulse. Postprocessor computations predict that seeding such an amplifier with 0.5 nJ HH pulses at 5 mrad grazing incidence would result in soft x-ray laser pulses of 290 fs duration (lower curve in Fig. 4).

In conclusion, we have measured the duration of laser pulses generated by an injection-seeded dense plasma soft x-ray laser amplifier generated by irradiation of a solid target. The measured pulse duration of 1.13 ± 0.47 ps is the shortest generated to date by a soft x-ray plasma amplifier. Injection seeding of plasma amplifiers creates a fundamentally unique regime for the generation of short soft x-ray laser pulses in which the pulse duration is independent of the gain duration. Simulations suggest that injection seeding of denser plasma amplifiers should make possible the generation of phase-coherent soft x-ray laser pulses of a few hundred femtosecond duration. These high brightness ultrafast table-top soft x-ray lasers will make possible the diagnostics of very rapidly evolving laser-created plasmas near the critical surface, ultrafast imaging with nanometer-scale resolution, and other ultrafast dynamic applications requiring a large number of photons per pulse.

This work was supported by the NSF Center for Extreme Ultraviolet Science and Technology under NSF Grant Nos. EEC-0310717 and ECS-9977677, and the Chemical Sciences, Geosciences and Biosciences Division, Office of Basic Energy Sciences, Office of Science, U.S. Department of Energy, and the NSF under Grant No. 0457269. M.B. acknowledges support from DOE CSGF under Grant No. DE-FG02-97ER25308.

[1] J. Filevich *et al.*, Phys. Rev. Lett. **94**, 035005 (2005).
[2] R. F. Smith, J. Dunn, J. Nilsen, V. N. Shlyaptsev, S. Moon, J. Filevich, J. J. Rocca, M. C. Marconi, J. R. Hunter, and T. W. Barbee, Phys. Rev. Lett. **89**, 065004 (2002).
[3] S. Suckewer and C. H. Skinner, Science **247**, 1553 (1990).
[4] G. Vaschenko *et al.*, Opt. Lett. **31**, 1214 (2006).
[5] R. Z. Tai, K. Namikawa, A. Sawada, M. Kishimoto, M. Tanaka, P. Lu, K. Nagashima, H. Maruyama, and M. Ando, Phys. Rev. Lett. **93**, 087601 (2004).
[6] P. W. Wachulak *et al.*, Opt. Express **15**, 3465 (2007).
[7] A. J. Nelson, J. Dunn, T. van Buuren, and J. Hunter, Appl. Phys. Lett. **85**, 6290 (2004).
[8] F. Dong, S. Heinbuch, J. J. Rocca, and E. R. Bernstein, J. Chem. Phys. **125**, 154317 (2006).
[9] S. Namba, N. Hasegawa, M. Nishikino, T. Kawachi, M. Kishimoto, K. Sukegawa, M. Tanaka, Y. Ochi, K. Takiyama, and K. Nagashima, Phys. Rev. Lett. **99**, 043004 (2007).
[10] P. V. Nickles, V. N. Shlyaptsev, M. Kalachnikov, M. Schnurer, I. Will, and W. Sandner, Phys. Rev. Lett. **78**, 2748 (1997).
[11] J. Dunn *et al.* Proc. SPIE **5197**, 51 (2003); J. Dunn, Y. Li, A. L. Osterheld, J. Nilsen, J. R. Hunter, and V. N. Shlyaptsev, Phys. Rev. Lett. **84**, 4834 (2000).
[12] A. Klisnick *et al.*, Phys. Rev. A **65**, 033810 (2002).
[13] Y. Abou-Ali *et al.*, Opt. Commun. **215**, 397 (2003).
[14] M. A. Larotonda *et al.*, Opt. Lett. **31**, 3043 (2006).
[15] Ph. Zeitoun *et al.*, Nature (London) **431**, 426 (2004).
[16] Y. Wang, E. Granados, M. A. Larotonda, M. Berrill, B. M. Luther, D. Patel, C. S. Menoni, and J. J. Rocca, Phys. Rev. Lett. **97**, 123901 (2006).
[17] Y. Wang *et al.*, Nat. Photonics **2**, 94 (2008).
[18] N. Hasegawa *et al.*, Phys. Rev. A **76**, 043805 (2007).
[19] F. Pedaci *et al.*, Opt. Lett. **33**, 491 (2008).
[20] I. R. Al'miev, O. Larroche, D. Benredjem, J. Dubau, S. Kazamias, C. Möller, and A. Klisnick, Phys. Rev. Lett. **99**, 123902 (2007).
[21] M. M. Shakya and Z. Chang, Appl. Phys. Lett. **87**, 041103 (2005).
[22] D. Alessi *et al.*, Opt. Express **13**, 2093 (2005).
[23] R. Keenan, J. Dunn, P. K. Patel, D. F. Price, R. F. Smith, and V. N. Shlyaptsev, Phys. Rev. Lett. **94**, 103901 (2005).
[24] Y. Wang, M. A. Larotonda, B. M. Luther, D. Alessi, M. Berrill, V. N. Shlyaptsev, and J. J. Rocca, Phys. Rev. A **72**, 053807 (2005).
[25] M. A. Berrill, M.S. thesis, Colorado State University, 2006.